

NMDA-Induced Calcium Loads Recycle Across the Mitochondrial Inner Membrane of Hippocampal Neurons in Culture

GUANG JIAN WANG AND STANLEY A. THAYER

Department of Pharmacology, University of Minnesota Medical School, Minneapolis, Minnesota 55455-0217

Received 27 April 2001; accepted in final form 15 October 2001

Wang, Guang Jian and Stanley A. Thayer. NMDA-induced calcium loads recycle across the mitochondrial inner membrane of hippocampal neurons in culture. *J Neurophysiol* 87: 740–749, 2002; 10.1152/jn.00345.2001. Mitochondria sequester *N*-methyl-D-aspartate (NMDA)-induced Ca^{2+} loads and regulate the shape of intracellular Ca^{2+} concentration ($[\text{Ca}^{2+}]_i$) responses in neurons. When isolated mitochondria are exposed to high $[\text{Ca}^{2+}]_i$, Ca^{2+} enters the matrix via the uniporter and returns to the cytosol by $\text{Na}^+/\text{Ca}^{2+}$ exchange. Released Ca^{2+} may re-enter the mitochondrion recycling across the inner membrane dissipating respiratory energy. Ca^{2+} recycling, the continuous uptake and release of Ca^{2+} by mitochondria, has not been described in intact neurons. Here we used single-cell microfluorimetry to measure $[\text{Ca}^{2+}]_i$ and mitochondrially targeted aequorin to measure matrix Ca^{2+} concentration ($[\text{Ca}^{2+}]_{\text{mt}}$) to determine whether Ca^{2+} recycles across the mitochondrial inner membrane in intact neurons following treatment with NMDA. We used ruthenium red and CGP 37157 to block uptake via the uniporter and release via $\text{Na}^+/\text{Ca}^{2+}$ exchange, respectively. As predicted by the Ca^{2+} recycling hypothesis, blocking the uniporter immediately following challenge with 200 μM NMDA produced a rapid and transient increase in cytosolic Ca^{2+} without a corresponding increase in matrix Ca^{2+} . Blocking mitochondrial Ca^{2+} release produced the opposite effect, depressing cytosolic Ca^{2+} levels and prolonging the time for matrix Ca^{2+} levels to recover. The Ca^{2+} recycling hypothesis uniquely predicts these reciprocal changes in the Ca^{2+} levels between the two compartments. Ca^{2+} recycling was not detected following treatment with 20 μM NMDA. Thus Ca^{2+} recycling across the inner membrane was more pronounced following treatment with a high relative to a low concentration of NMDA, consistent with a role in Ca^{2+} -dependent neurotoxicity.

INTRODUCTION

Mitochondria are able to sequester large amounts of Ca^{2+} (Blaustein et al. 1978; Gunter et al. 1994; Lehninger 1967) and thus regulate the shape of $[\text{Ca}^{2+}]_i$ responses in neurons (David 1999; Friel and Tsien 1994; Tang and Zucker 1997; Thayer and Miller 1990; Werth and Thayer 1994), including neurons stimulated with glutamate and NMDA (Nicholls and Ward 2000; Peng and Greenamyre 1998; Wang and Thayer 1996; White and Reynolds 1995). Ca^{2+} is taken up by mitochondria via a ruthenium-red-sensitive uniporter driven by the proton electrochemical gradient ($\Delta\Psi = -180$ mV). Ca^{2+} exits the mitochondrion via a $\text{Na}^+/\text{Ca}^{2+}$ exchange process, and Na^+ is removed from the matrix

by Na^+/H^+ exchange. Thus there are separate routes for Ca^{2+} uptake and release, both driven by $\Delta\Psi$ present on the inner membrane (Nicholls and Ferguson 1992).

Ca^{2+} uptake into the mitochondrion has numerous consequences (Duchen 1999). Increases in $[\text{Ca}^{2+}]_{\text{mt}}$ stimulate the tricarboxylic acid cycle coupling energy demand to ATP production (McCormack et al. 1990). Elevated $[\text{Ca}^{2+}]_{\text{mt}}$ may open the mitochondrial permeability transition pore, producing Ca^{2+} -induced Ca^{2+} -release from mitochondria or, in the high-conductance mode, cell death (Ichas and Mazat 1998; Miller 1998). Sequestration of Ca^{2+} into mitochondria buffers potentially toxic Ca^{2+} loads, although it may also produce deleterious effects (Castilho et al. 1999; Stout et al. 1998). Increases in $[\text{Ca}^{2+}]_{\text{mt}}$ accelerates electron transport (McCormack et al. 1990) and stimulates the production of reactive oxygen species (Castilho et al. 1999; Chacon and Acosta 1991). Released Ca^{2+} may re-enter the mitochondrion potentially setting up a futile Ca^{2+} cycle across the inner mitochondrial membrane. The simultaneous uptake and release of Ca^{2+} , defined here as Ca^{2+} recycling, has been described in studies with isolated mitochondria (Crompton et al. 1976) where it was shown to dissipate respiratory energy (Crompton and Heid 1978). Sequential movement of Ca^{2+} through the mitochondrial Ca^{2+} cycle (uniporter \rightarrow matrix \rightarrow $\text{Na}^+/\text{Ca}^{2+}$ exchange) has been observed in intact neurons (Friel and Tsien 1994; Werth and Thayer 1994), but Ca^{2+} re-cycling across the inner membrane has not been described. Because mitochondria in situ are in close contact with endoplasmic reticulum (Rizzuto et al. 1998) and plasmalemma (Montero et al. 2000) Ca^{2+} channels, they may experience extremely high Ca^{2+} and Na^+ concentrations that promote Ca^{2+} recycling.

We determined whether Ca^{2+} recycling occurs in intact hippocampal neurons challenged with *N*-methyl-D-aspartate (NMDA). Changes in both $[\text{Ca}^{2+}]_i$ and $[\text{Ca}^{2+}]_{\text{mt}}$ were measured directly, enabling us to determine whether NMDA-induced Ca^{2+} loads shifted between the mitochondrial and cytosolic compartments. Pharmacological blockade of Ca^{2+} fluxes across the inner membrane elicited reciprocal changes in $[\text{Ca}^{2+}]_{\text{mt}}$ and $[\text{Ca}^{2+}]_i$ that were consistent with Ca^{2+} recycling across the mitochondrial inner membrane following exposure to high concentrations of NMDA.

Address for reprint requests: S. A. Thayer, Dept. of Pharmacology, University of Minnesota Medical School, 6-120 Jackson Hall, 321 Church St. SE, Minneapolis, MN 55455-0217 (E-mail: thayer@med.umn.edu).

The costs of publication of this article were defrayed in part by the payment of page charges. The article must therefore be hereby marked "advertisement" in accordance with 18 U.S.C. Section 1734 solely to indicate this fact.

METHODS

Materials

Materials were obtained from the following suppliers: Indo-1 and Indo-5F, Molecular Probes, Eugene OR; Dulbecco's modified Eagle's medium and B27 supplement, GIBCO, Grand Island, NY; heat-inactivated iron supplemented calf serum, Hyclone Laboratories, Logan, UT; NuSerum IV, Collaborative Research, Bedford, MA; superoxide dismutase, Boehringer-Mannheim Biochemicals, Indianapolis, IN; SMI 81 and SMI 311, Sternberger Monoclonals, Baltimore, MD; Ham's F-12, catalase, tetrodotoxin and all other reagents, Sigma/RBI, St. Louis, MO.

Cell culture

Astrocyte-poor, neuron-rich hippocampal cultures were prepared using methods similar to those described previously (Wang et al. 1994, 1998). Fetuses were removed on embryonic day 17 from maternal Sprague-Dawley rats anesthetized with CO_2 and killed by decapitation. Hippocampi were dissected and placed in Ca^{2+} and Mg^{2+} -free *N*-2-hydroxyethylpiperazine-*N'*-2-ethanesulfonic acid (HEPES)-buffered Hanks' salt solution (HHSS), pH 7.45. HHSS was composed of the following (in mM): 20 HEPES, 137 NaCl, 1.3 CaCl_2 , 0.4 MgSO_4 , 0.5 MgCl_2 , 5.0 KCl, 0.4 KH_2PO_4 , 0.6 Na_2HPO_4 , 3.0 NaHCO_3 , and 5.6 glucose. Cells were dissociated by triturating through a 5-ml pipette and then a flame-narrowed Pasteur pipette. The neurons were grown in a humidified atmosphere of 10% CO_2 -90% air at 37°C. Cultures were initially plated at a density of 100,000 cells per well onto 25-mm round coverglasses (#1) that had been coated with poly-D-lysine (0.1 mg/ml) and washed with H_2O . The initial medium was an 80:10:10 (vol/vol) mixture of Dulbecco's modified Eagle's medium, Ham's F-12, and heat-inactivated iron supplemented calf serum, containing 2 mM glutamine, 25 mM HEPES, 24 units/ml penicillin, and 24 $\mu\text{g}/\text{ml}$ streptomycin. After 24 h in vitro, cell proliferation was inhibited by the addition of 5 μM cytosine arabinoside to the media. On the third day of culture, the medium was completely removed and replaced with 90% minimal essential medium, 10% NuSerum IV, 2 mM glutamine, 5 mM HEPES, containing 10 $\mu\text{g}/\text{ml}$ superoxide dismutase, 1 $\mu\text{g}/\text{ml}$ catalase, 11 mM total glucose, and 9.3 mM total sodium bicarbonate, plus 2% B27 supplement. Medium was not changed subsequently. To prevent evaporation of water, culture dishes were kept on "wet dishes" containing a filter paper that was always kept wet. Cells were used after they were in culture for 11–15 days. Cultures were characterized using immunocytochemical methods as previously described (Wang et al. 1998). The percentage of astrocytes in these cultures was determined by counting cell nuclei, labeled with bisbenzamide, yielding total cells, and GFAP-positive cells (astrocytes) in five randomly chosen optical fields ($\times 20$ objective) per coverslip using cultures at 2–3 wk. Seventy-nine GFAP-positive cells were found among the 4,534 cells counted in three separate experiments (1–3 coverslips per experiment). Thus these cultures contained $\sim 2\%$ astrocytes. Neurons were positively identified using a cocktail of antineurofilament monoclonal antibodies, SMI 81 and SMI 311. In three separate experiments (total of 6 coverslips), we found that $94 \pm 1\%$ (mean \pm SE) of total cells were positively labeled by the anti-neurofilament antibody cocktail. The rest of cells in these experiments were either astrocytes or neurons that could not be positively identified because they were in an aggregate or were weakly labeled.

 $[\text{Ca}^{2+}]_i$ measurement

Cells were loaded with Indo-1 or Indo-5F by incubation in 2 μM of the acetoxymethyl ester form of the dye for 45 min at 37°C in HHSS containing 0.5% bovine serum albumin. Coverslips with loaded cells were mounted in a flow-through chamber for viewing (Thayer et al. 1988). The superfusion chamber was mounted on an inverted micro-

scope and cells were superfused with HHSS at a rate of 1–2 ml/min for 15 min prior to starting an experiment. The bath was completely exchanged within 10 s. $[\text{Ca}^{2+}]_i$ was determined with a previously described dual-emission microfluorimeter (Wang and Thayer 1996). The optical settings for Indo-1 and Indo-5F were the same. For excitation, the light from a 75-W xenon arc lamp was passed through a 350 (10)-nm band-pass filter (Omega Optical, Brattleboro, VT), reflected off of a dichroic mirror (380 nm) and through a X70 phase-contrast oil-immersion objective (Leitz, numerical aperture 1.15). Emitted light was sequentially reflected off of dichroic mirrors (440 and 516 nm) through band-pass filters [405 (20) and 495 (20) nm, respectively] to photomultiplier tubes operating in photon-counting mode (Thorn EMI, Fairfield, NJ). Cells were illuminated with transmitted light (580-nm long pass) and visualized with a video camera placed after the second emission dichroic. Recordings were defined spatially with a rectangular diaphragm. The 5-V photomultiplier output was integrated by passing the signal through an eight-pole Bessel filter at 2.5 Hz. This signal was then input into two channels of an A/D converter (Indec Systems, Sunnyvale, CA) sampling at 1 Hz.

After completion of each experiment, the microscope stage was adjusted so that no cells or debris occupied the field of view defined by the diaphragm, and the background light levels were determined (typically $<5\%$ of cell counts). Autofluorescence from cells that were not loaded with dye was undetectable. Records were later corrected for background and converted to $[\text{Ca}^{2+}]_i$ by the equation $[\text{Ca}^{2+}]_i = K_d\beta(R - R_{\min})/(R_{\max} - R)$, in which R is the 405/495-nm fluorescence ratio. The dissociation constants (K_d) used for Indo-1 and Indo-5F were 225 and 473 nM, respectively, and β was the ratio of emitted fluorescence at 495 nm in the absence and presence of calcium. R_{\min} , R_{\max} , and β were determined in ionomycin-permeabilized cells in calcium-free (1 mM EGTA) and 5 mM Ca^{2+} buffers. Values of R_{\min} , R_{\max} , and β for Indo-1 were 0.25, 2.3, and 3.5, and for Indo-5F were 0.21, 1.64, and 4.5, respectively.

 $[\text{Ca}^{2+}]_{mi}$ measurement

Measurement of intramitochondrial Ca^{2+} ($[\text{Ca}^{2+}]_{mi}$) was achieved using the Ca^{2+} -sensitive photoprotein aequorin targeted to the mitochondrion of hippocampal neurons (Cobbold and Lee 1991; Padua et al. 1998; Rizzuto et al. 1993). The apoaquorin gene fused to the mitochondrial targeting sequence from subunit VIII of cytochrome C oxidase (COXVIII) was excised from plasmid mtAeq-pMT2 (Rizzuto et al. 1993). The gene was inserted into shuttle plasmid pAdRSV4 behind the RSV promoter (Bohn et al. 1999). The RSVmtAeq expression cassette was then incorporated into a recombinant adenovirus by the Gene Transfer Vector Core at the University of Iowa.

After 11–15 days in culture, hippocampal neurons were infected with adenovirus carrying the mitochondrial apoaquorin expression construct by adding 0.3×10^{10} to 1×10^{10} viral particles to each culture well in 1.5 ml medium and incubated at 37°C. After 24 h, the infection medium was removed and the cells were washed in the same volume of growth medium overnight. The apoaquorin protein was reconstituted to form aequorin by incubating transfected cells in serum-free DMEM containing 5 μM coelenterazine *f* at 37°C for 1–1.5 h prior to the experiment.

The custom-built luminescence detection system employed here was described previously (Padua et al. 1998). After the apoaquorin protein was reconstituted to aequorin, a coverslip with attached neurons was mounted in a stainless steel perfusion chamber and raised to within 10 mm of an inverted photomultiplier tube (Thorn Instruments). The cells were superfused with HHSS for ≥ 10 min prior to starting the experiment to wash out any excess coelenterazine. Luminescence was quantified with a Thorn EMI CT 1 counting board installed in a microcomputer sampling at 1 Hz.

On binding Ca^{2+} , aequorin emits a photon and its coelenterazine prosthetic group is irreversibly oxidized, rendering the aequorin incapable of further luminescent reactions with Ca^{2+} . Thus increasing

Ca^{2+} levels will increase the rate of aequorin decay. To correct for the consumption of aequorin, neurons were lysed at the end of the experiment in H_2O containing 12.6 mM Ca^{2+} to discharge any remaining aequorin. Total aequorin counts available during the experiment were determined by integrating photon counts over the entire experiment including lysis. This enabled calculating the fractional rate of aequorin decay (α) from the equation $\alpha = (\text{photon counts/s})/\text{counts remaining}$ (Cobbold and Lee 1991). The $-\log(\alpha)$ is proportional to $\log[\text{Ca}^{2+}]_{\text{mt}}$ and was thus used to report changes in $[\text{Ca}^{2+}]_{\text{mt}}$, although the indicator was not calibrated for absolute values of $[\text{Ca}^{2+}]_{\text{mt}}$. $[\text{Ca}^{2+}]_{\text{mt}}$ recordings were filtered digitally with a three-point moving average.

RESULTS

NMDA-induced changes in $[\text{Ca}^{2+}]_i$ and $[\text{Ca}^{2+}]_{\text{mt}}$

Changes in $[\text{Ca}^{2+}]_i$ were induced in hippocampal neurons grown in primary culture by 60-s exposure to either high (200 μM) or low (20 μM) concentrations of NMDA and measured with either the high-affinity Ca^{2+} indicator, Indo-1 ($K_d = 225$ nM) or the low-affinity Ca^{2+} indicator, Indo-5F ($K_d = 473$ nM). Peak $[\text{Ca}^{2+}]_i$ values induced by 20 μM NMDA were similar regardless of whether they were recorded with Indo-1 or Indo-5F. The peak 20 μM NMDA-induced $[\text{Ca}^{2+}]_i$ increase reported by Indo-1 was 518 ± 47 nM ($n = 6$), and the peak value measured with Indo-5F was 517 ± 128 nM ($n = 6$). With 200 μM NMDA, the amplitude of the $[\text{Ca}^{2+}]_i$ increase reported by Indo-5F tended to be greater than that reported by Indo-1. Indo-1 reported an increase in $[\text{Ca}^{2+}]_i$ of 818 ± 211 nM ($n = 6$), and Indo-5F reported an increase of $1,396 \pm 392$ nM ($n = 5$). The difference between Indo-1 and Indo-5F in the measurement of large increases of $[\text{Ca}^{2+}]_i$ was more pronounced when cells were stimulated with 200 μM NMDA in the presence of 1 μM carbonyl cyanide p-(trifluoromethoxy) phenylhydrazone (FCCP) plus 1 μM oligomycin, a treatment that increases the amplitude of NMDA-induced $[\text{Ca}^{2+}]_i$ responses (Wang and Thayer 1996). Following this treatment, Indo-1 reported an increase in $[\text{Ca}^{2+}]_i$ to $1,122 \pm 209$ nM ($n = 10$), and Indo-5F measured a significantly larger increase to $2,017 \pm 424$ nM ($n = 6$; $P < 0.05$). These results indicated that Indo-5F was a more suitable indicator than Indo-1 for the measurement of large increases in $[\text{Ca}^{2+}]_i$, such as those elicited by 200 μM NMDA. Accordingly, in the following experiments, we used Indo-1 to measure 20 μM NMDA-induced $[\text{Ca}^{2+}]_i$ changes and Indo-5F to measure 200 μM NMDA-induced $[\text{Ca}^{2+}]_i$ changes.

Direct measurement of the calcium concentration within the mitochondrial matrix was achieved by transferring the apoaequorin gene fused to a mitochondrial targeting sequence to hippocampal neurons with an adenoviral vector. A similar approach was used to successfully report $[\text{Ca}^{2+}]_{\text{mt}}$ in histamine/ATP-stimulated Hela cells (Rizzuto et al. 1998), in pyruvate dehydrogenase-deficient human fibroblasts (Padua et al. 1998), and in chromaffin cells stimulated by depolarization (Montero et al. 2000). Here we used this technique to record intramitochondrial calcium changes in primary cultures of hippocampal neurons stimulated with NMDA. Figure 1, A and B, shows $[\text{Ca}^{2+}]_{\text{mt}}$ responses induced by 20 and 200 μM NMDA, respectively. Corresponding single-cell $[\text{Ca}^{2+}]_i$ responses are shown in Fig. 1, C and D. The shape of the $[\text{Ca}^{2+}]_i$ and $[\text{Ca}^{2+}]_{\text{mt}}$ waveforms were similar. Because $[\text{Ca}^{2+}]_i$ was mea-

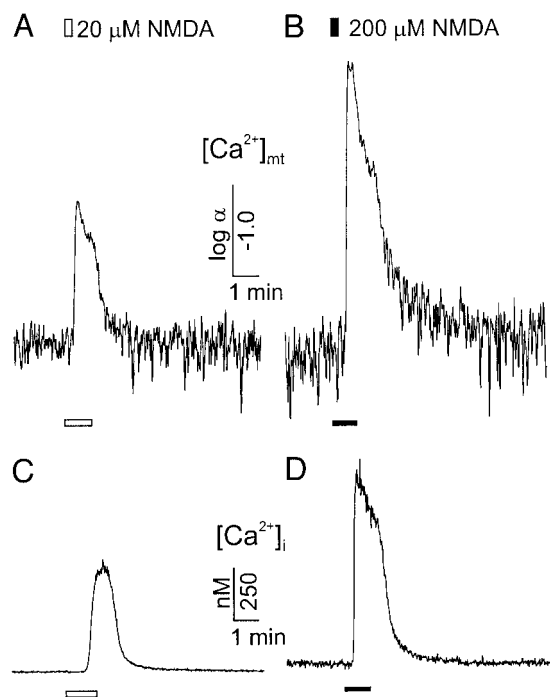


FIG. 1. N-methyl-D-aspartate (NMDA)-induced changes in $[\text{Ca}^{2+}]_i$ and $[\text{Ca}^{2+}]_{\text{mt}}$ in cultures of hippocampal neurons. A and B: $[\text{Ca}^{2+}]_{\text{mt}}$ responses were induced by 60-s exposure to 20 or 200 μM NMDA as indicated by \square and \blacksquare , respectively. Intramitochondrial Ca^{2+} changes were recorded in populations of hippocampal neurons using the mitochondrially targeted aequorin-based luminescent technique described in METHODS. $[\text{Ca}^{2+}]_{\text{mt}}$ is presented as $-\log \alpha$ which is proportional to $\log[\text{Ca}^{2+}]_{\text{mt}}$. C and D: $[\text{Ca}^{2+}]_i$ responses induced by 60-s exposure to 20 and 200 μM NMDA. The 20 μM NMDA-induced $[\text{Ca}^{2+}]_i$ response was recorded using the high-affinity Ca^{2+} indicator, Indo-1. The 200 μM NMDA-induced $[\text{Ca}^{2+}]_i$ response was recorded using the low-affinity Ca^{2+} indicator, Indo-5F. $[\text{Ca}^{2+}]_i$ was recorded and calibrated as described in METHODS. Traces are representative of 5 recordings.

sured in single cells and $[\text{Ca}^{2+}]_{\text{mt}}$ was recorded from a population of cells, an exact temporal comparison of these two types of responses was not attempted, although the recording chamber and the method of drug application for both instruments were identical. In experiments in which 200 and 20 μM NMDA were applied during the same recording, the high concentration of NMDA produced a significantly greater increase in $[\text{Ca}^{2+}]_i$ (200 μM response/20 μM response = 1.68 ± 0.15 , $n = 5$) and $[\text{Ca}^{2+}]_{\text{mt}}$ (200 μM response/20 μM response = 1.7 ± 0.3 , $n = 7$; $P < 0.05$, paired t -test).

FCCP blocked NMDA-induced $[\text{Ca}^{2+}]_{\text{mt}}$ changes and enhanced $[\text{Ca}^{2+}]_i$ responses

Cells were treated with the mitochondrial poisons FCCP and oligomycin to provide a functional assessment of the targeting of aequorin to mitochondria. Exposing hippocampal neurons to 200 μM NMDA for 1 min at 10- to 15-min intervals elicited reproducible increases in $[\text{Ca}^{2+}]_i$ (Fig. 2A) and $[\text{Ca}^{2+}]_{\text{mt}}$ (Fig. 2C). The second $[\text{Ca}^{2+}]_i$ response was $92 \pm 4\%$ ($n = 5$) of the first and the second $[\text{Ca}^{2+}]_{\text{mt}}$ response $86 \pm 5\%$ ($n = 6$) of the initial response. Pretreatment with 1 μM FCCP and 1 μM oligomycin for 5 min inhibited the mitochondrial response by $56 \pm 6\%$ ($n = 6$, $P < 0.01$; Fig. 2D), but enhanced the $[\text{Ca}^{2+}]_i$ response by approximately twofold (Fig. 2B). The $[\text{Ca}^{2+}]_i$ increase induced by the first 200 μM NMDA stimulus was

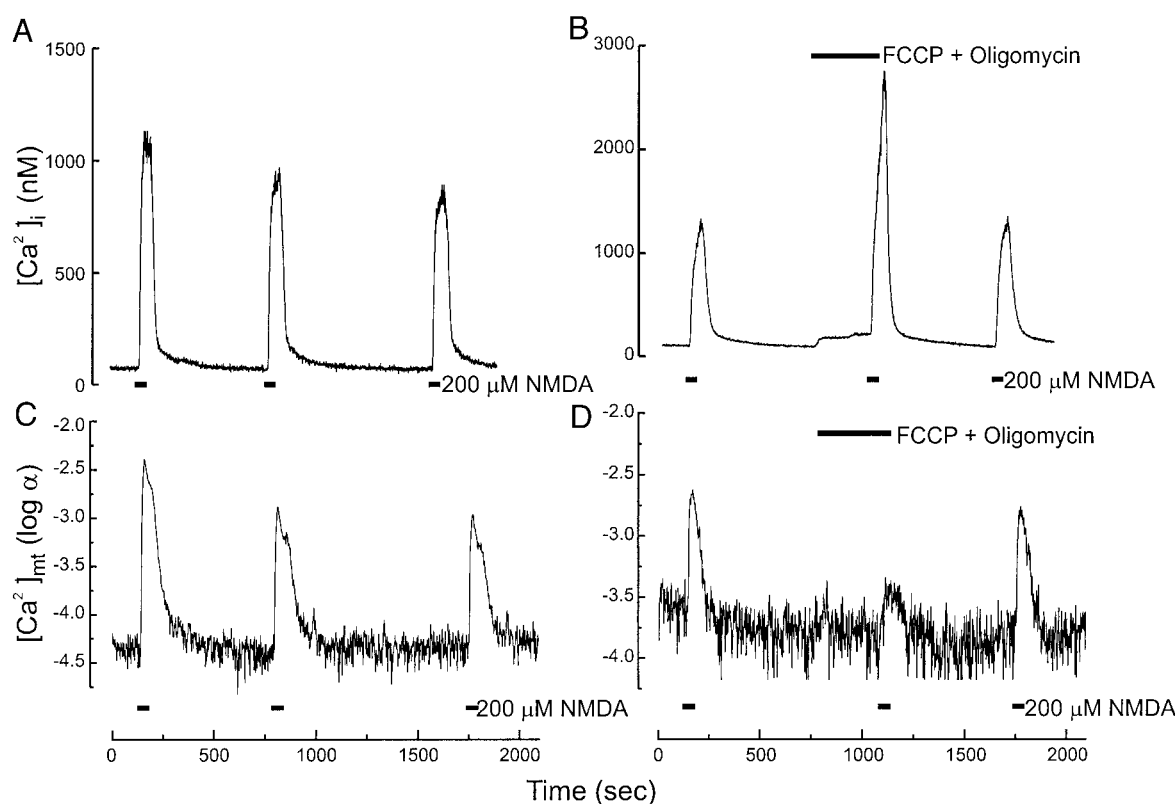


FIG. 2. Carbonyl cyanide p-(trifluoro-methoxy) phenylhydrazone (FCCP) increased the amplitude of $[\text{Ca}^{2+}]_i$ responses but decreased the amplitude of $[\text{Ca}^{2+}]_{mt}$ responses in hippocampal neurons stimulated with $200 \mu\text{M}$ NMDA. **A** and **C**: $200 \mu\text{M}$ NMDA-induced $[\text{Ca}^{2+}]_i$ and $[\text{Ca}^{2+}]_{mt}$ responses in control cells. The NMDA stimulus was applied for 1 min at the time indicated (■). **B** and **D**: pretreatment with $1 \mu\text{M}$ FCCP plus $1 \mu\text{M}$ oligomycin for 5 min enhanced the $[\text{Ca}^{2+}]_i$ response, but inhibited the $[\text{Ca}^{2+}]_{mt}$ response induced by $200 \mu\text{M}$ NMDA. $[\text{Ca}^{2+}]_i$ was measured using the low-affinity Ca^{2+} indicator Indo-5F. $[\text{Ca}^{2+}]_{mt}$ was recorded as described in METHODS. Note that a small elevation in $[\text{Ca}^{2+}]_i$ induced by $1 \mu\text{M}$ FCCP plus $1 \mu\text{M}$ oligomycin in **B** was not accompanied by an increase in the corresponding $[\text{Ca}^{2+}]_{mt}$ trace in **D**. Traces are representative of 5–6 recordings.

$849 \pm 145 \text{ nM}$, and in the presence of FCCP plus oligomycin, the NMDA-induced $[\text{Ca}^{2+}]_i$ response increased to a peak value of $2,017 \pm 424 \text{ nM}$ ($n = 6$, $P < 0.01$). In addition, FCCP and oligomycin produced a small increase in basal $[\text{Ca}^{2+}]_i$ to $193 \pm 26 \text{ nM}$ ($n = 6$) when applied to these cells. This increase in $[\text{Ca}^{2+}]_i$ was not accompanied by an increase in $[\text{Ca}^{2+}]_{mt}$ (Fig. 2, **B** and **D**).

Twenty micromolar NMDA also elicited three reproducible $[\text{Ca}^{2+}]_i$ (Fig. 3A) and $[\text{Ca}^{2+}]_{mt}$ (Fig. 3C) responses in hippocampal neurons. The second $[\text{Ca}^{2+}]_i$ response was $90 \pm 2\%$ ($n = 6$) of the first, and the second $[\text{Ca}^{2+}]_{mt}$ response was $93 \pm 4\%$ ($n = 5$) of the first. FCCP plus oligomycin enhanced the $[\text{Ca}^{2+}]_i$ response induced by $20 \mu\text{M}$ NMDA by $78 \pm 30\%$ ($n = 5$, $P < 0.01$; Fig. 3B). The $[\text{Ca}^{2+}]_i$ increase evoked by the first $20 \mu\text{M}$ NMDA stimulus was $412 \pm 87 \text{ nM}$, and in the presence of FCCP and oligomycin, $[\text{Ca}^{2+}]_i$ reached a peak value of $765 \pm 143 \text{ nM}$. FCCP inhibited the $20 \mu\text{M}$ NMDA-induced $[\text{Ca}^{2+}]_{mt}$ response by $75 \pm 8\%$ ($n = 6$, $P < 0.01$; Fig. 3D).

Mitochondrial $\text{Na}^+/\text{Ca}^{2+}$ exchange was pronounced following large but not small Ca^{2+} loads

CGP 37157 inhibits $\text{Na}^+/\text{Ca}^{2+}$ exchange across the inner mitochondrial membrane (Cox et al. 1993). This drug also has some Ca^{2+} channel blocking activity; thus for selective effects on mitochondria, it was found that application after the stim-

ulus altered $[\text{Ca}^{2+}]_i$ recovery kinetics in a manner consistent with slowed release of Ca^{2+} from the mitochondrial matrix (Baron and Thayer 1997; White and Reynolds 1997).

In this set of experiments, we used a similar protocol to study the effects of CGP 37157 on NMDA-induced changes in $[\text{Ca}^{2+}]_i$ and $[\text{Ca}^{2+}]_{mt}$. Application of $3 \mu\text{M}$ CGP 37157 for 3 min following the NMDA stimulus did not significantly affect the amplitude of the $200 \mu\text{M}$ NMDA-induced $[\text{Ca}^{2+}]_i$ response. The amplitude of the second response normalized to the first response in control cells was $92 \pm 4\%$ ($n = 5$; Fig. 2A) versus $89 \pm 2\%$ ($n = 5$) in CGP 37157-treated cells (Fig. 4A). CGP 37157 reduced the duration of the recovery phase that followed $200 \mu\text{M}$ NMDA-induced $[\text{Ca}^{2+}]_i$ increases (Fig. 4A). The recovery phase was quantified by measuring the width of the response at 15% of the net $[\text{Ca}^{2+}]_i$ increase (horizontal line in Fig. 4A). Relative to the initial response ($125 \pm 17 \text{ s}$), the width was significantly reduced ($P < 0.01$) in CGP 37157-treated cells ($102 \pm 8 \text{ s}$; Fig. 4A), consistent with the idea that Ca^{2+} release from mitochondria contributed to the $[\text{Ca}^{2+}]_i$ during recovery. Removal of CGP 37157 caused an immediate rise in $[\text{Ca}^{2+}]_i$ (Fig. 4A), suggesting that Ca^{2+} trapped within the mitochondria was released on removal of the drug. The amplitude of this $[\text{Ca}^{2+}]_i$ transient was $65 \pm 33 \text{ nM}$ ($n = 5$), and it recovered slowly during a subsequent 10-min wash period (Fig. 4A). This secondary rise in $[\text{Ca}^{2+}]_i$ was not observed in control experiments ($n = 5$; Fig. 2A).

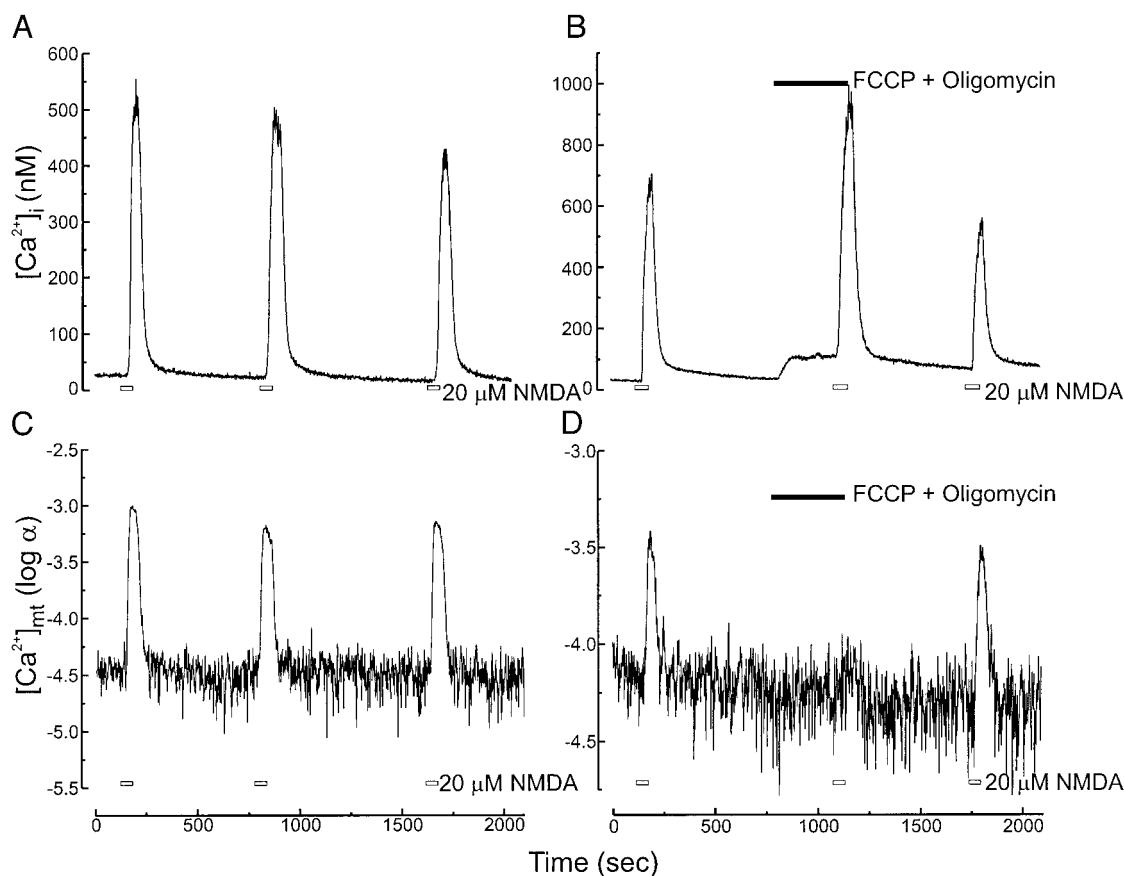


FIG. 3. Opposite effects of FCCP on $[Ca^{2+}]_i$ and $[Ca^{2+}]_{mt}$ in hippocampal neurons exposed to 20 μ M NMDA. *A* and *C*: 20 μ M NMDA-induced $[Ca^{2+}]_i$ and $[Ca^{2+}]_{mt}$ responses in control cells. NMDA was applied for 1 min as indicated (\square). *B* and *D*: pretreatment with 1 μ M FCCP plus 1 μ M oligomycin for 5 min (\blacksquare) enhanced the $[Ca^{2+}]_i$, but inhibited the $[Ca^{2+}]_{mt}$ responses induced by 20 μ M NMDA. $[Ca^{2+}]_i$ responses were measured with Indo-1. Note the expanded $[Ca^{2+}]_i$ scale in this figure relative to that in Fig. 2. $[Ca^{2+}]_{mt}$ was recorded as described in METHODS. The small elevation in $[Ca^{2+}]_i$ induced by 1 μ M FCCP plus 1 μ M oligomycin in *B* was not accompanied by an increase in the corresponding $[Ca^{2+}]_{mt}$ recording in *D*. Traces are representative of 5–6 recordings.

Twenty micromolar NMDA also elicited three reproducible $[Ca^{2+}]_i$ responses (Fig. 4*B*). The $[Ca^{2+}]_i$ recovered to baseline more rapidly following 20 versus 200 μ M NMDA (compare Fig. 4, *B* with *A*). Application of 3 μ M CGP 37157 for 3 min had no effect on the amplitude of 20 μ M NMDA-induced $[Ca^{2+}]_i$ response which was $94 \pm 4\%$ ($n = 6$) of the initial control response (Fig. 3*A*). Drug treatment did not change the width of the Ca^{2+} recovery phase of the 20 μ M NMDA-induced $[Ca^{2+}]_i$ response (100 ± 10 s; $n = 6$) relative to the initial response (94 ± 8 s; $n = 6$), and removal of CGP 37157 did not produce a secondary rise in $[Ca^{2+}]_i$ ($n = 5$, Fig. 4*B*). Thus CGP 37157 altered $[Ca^{2+}]_i$ recovery kinetics following high but not low concentrations of NMDA.

Three consecutive applications of 200 μ M NMDA induced reproducible increases in $[Ca^{2+}]_{mt}$ (Fig. 2*C*). The amplitude of the second response was $86 \pm 5\%$ and its width $104 \pm 5\%$ relative to the first response ($n = 6$, $P > 0.05$). Application of 3 μ M CGP 37157 for 3 min immediately following the NMDA stimulus had no effect on the amplitude of the response, which peaked prior to drug application ($78 \pm 5\%$) and was similar to control ($86 \pm 5\%$). CGP 37157 prolonged the $[Ca^{2+}]_{mt}$ recovery (Fig. 4*C*). The width of the response was significantly longer in the presence of CGP 37157 (294 ± 52 s) relative to the initial response (154 ± 21 s; $n = 7$, $P < 0.01$; Fig. 4*C*).

Removal of CGP 37157 did not produce a detectable change in $[Ca^{2+}]_{mt}$ (Fig. 4*C*). Thus CGP 37157 exerted opposite effects on $[Ca^{2+}]_i$ and $[Ca^{2+}]_{mt}$; it accelerated the recovery of $[Ca^{2+}]_i$, but slowed the recovery of $[Ca^{2+}]_{mt}$.

Repetition of the preceding experiments with CGP 37157 in hippocampal neurons treated with 20 μ M NMDA showed that application of 3 μ M CGP 37157 for 3 min after the stimulus neither changed the amplitude nor the recovery of the $[Ca^{2+}]_{mt}$ response (Fig. 4*D*). The width in the absence of drug (96 ± 10 s, $n = 5$; Fig. 3*B*) was similar to that observed in the presence of CGP 37157 (85 ± 4 s, $n = 7$; Fig. 4*D*). No changes in $[Ca^{2+}]_{mt}$ were observed after CGP 37157 was removed (Fig. 4*D*). The lack of effect of CGP 37157 on $[Ca^{2+}]_{mt}$ and $[Ca^{2+}]_i$ responses elicited by 20 μ M NMDA suggests that the rate of Ca^{2+} efflux from the mitochondrion via Na^+/Ca^{2+} exchange was dependent on the size of the preceding Ca^{2+} load.

Blocking the mitochondrial Ca^{2+} uniporter increased $[Ca^{2+}]_i$ following 200 μ M but not 20 μ M NMDA

If Ca^{2+} was recycling across the inner mitochondrial membrane, then blocking Ca^{2+} uptake into mitochondria would be predicted to increase cytosolic Ca^{2+} . To test this hypothesis, we used ruthenium red, an effective inhibitor of the mitochon-

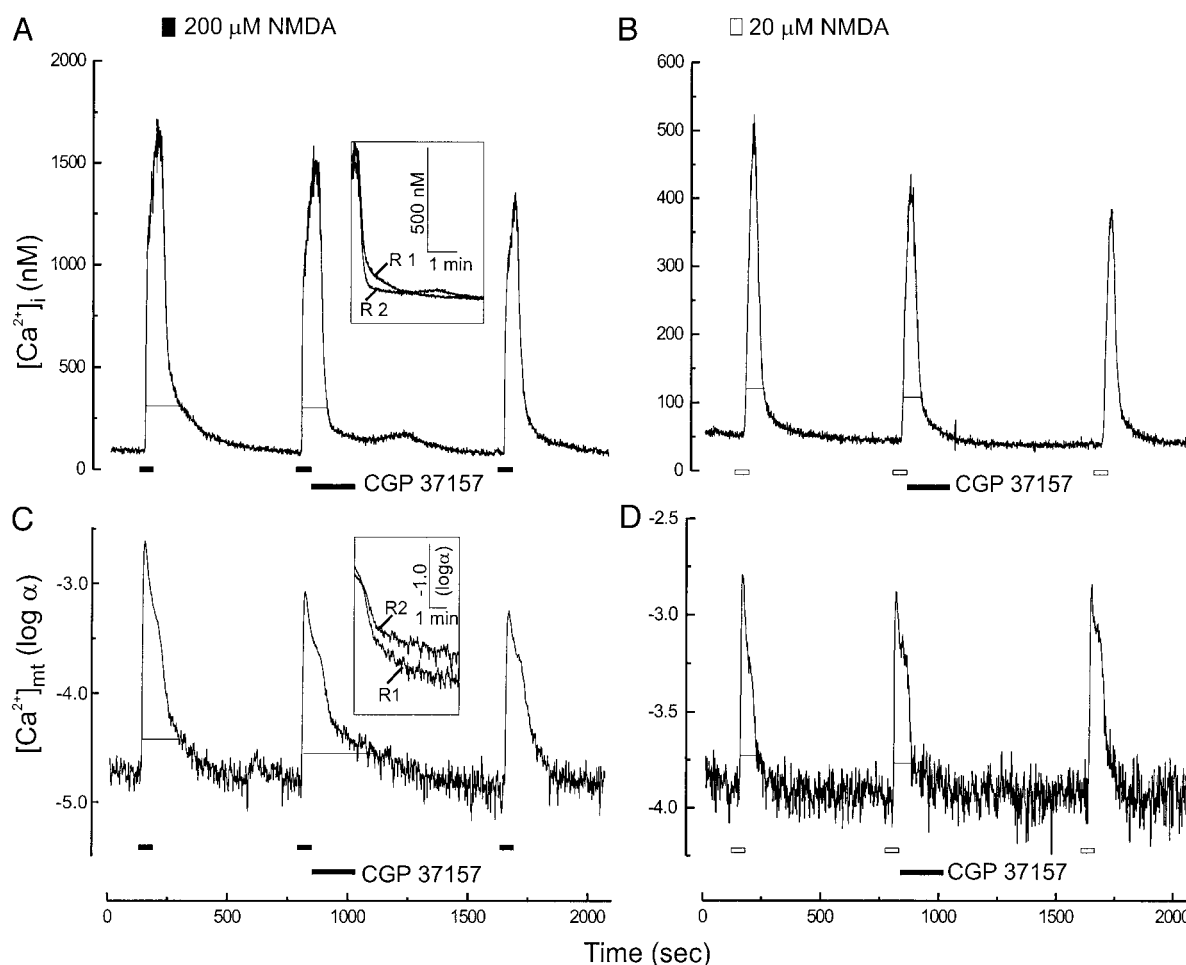


FIG. 4. Inhibition of mitochondrial $\text{Na}^+/\text{Ca}^{2+}$ exchange differentially affects recovery from small vs. large NMDA-induced Ca^{2+} loads in hippocampal neurons. **A:** application of $3 \mu\text{M}$ CGP 37157 for 3 min following $200 \mu\text{M}$ NMDA (60 s) accelerated the recovery of the $[\text{Ca}^{2+}]_i$ response. After CGP 37157 was removed, a secondary rise in $[\text{Ca}^{2+}]_i$ occurred due to the release of inhibition of mitochondrial $\text{Na}^+/\text{Ca}^{2+}$ exchange. **C:** CGP 37157 slowed the recovery of the $[\text{Ca}^{2+}]_{mt}$ response following $200 \mu\text{M}$ NMDA (60 s). A secondary rise in $[\text{Ca}^{2+}]_{mt}$ was absent in **C**. **Insets:** the recovery of response 1 (R1) and response 2 (R2) overlaid from the same recordings. **B** and **D:** CGP 37157 did not change the recovery kinetics of $[\text{Ca}^{2+}]_i$ and $[\text{Ca}^{2+}]_{mt}$ responses induced by $20 \mu\text{M}$ NMDA (60 s). The $[\text{Ca}^{2+}]_i$ responses induced by 20 and $200 \mu\text{M}$ NMDA were recorded using Indo-1 and Indo-5F, respectively. $[\text{Ca}^{2+}]_{mt}$ was recorded as described in METHODS. Horizontal lines indicate the width of the responses at 15% of net amplitude. Traces are representative of 5–6 recordings.

drial Ca^{2+} uniporter when applied to isolated mitochondria (Moore 1971). The use of this compound for inhibition of Ca^{2+} influx into mitochondria in intact cells is less straightforward. Several reports have effectively blocked changes in $[\text{Ca}^{2+}]_{mt}$ in intact cells with ruthenium red (Peng and Greenamyre 1998; Tan et al. 1998; Trollinger et al. 2000; Velasco and Tapia 2000), but interpretation of these results is complicated by the poor membrane permeability of this compound and its action on multiple Ca^{2+} entry pathways (Griffiths 2000; Malecot et al. 1998). The experiments described in the following text required the use of the rather high ruthenium red concentration of $100 \mu\text{M}$, presumably because of poor membrane permeability. Because this concentration would be expected to exert nonselective actions on Ca^{2+} entry pathways, we employed a protocol in which the drug was applied after the NMDA stimulus when Ca^{2+} entry had ceased. Note that any nonselective effects on Ca^{2+} channels would lower $[\text{Ca}^{2+}]_i$, in contrast to the increase predicted by the Ca^{2+} recycling hypothesis. Ruthenium red did not affect indicator fluorescence

as shown by analysis of the intensity values recorded during application of $100 \mu\text{M}$ ruthenium red.

Application of $100 \mu\text{M}$ ruthenium red for 3 min immediately following the $200 \mu\text{M}$ NMDA stimulus induced an immediate upstroke in $[\text{Ca}^{2+}]_i$ that exceeded the peak value of the NMDA-induced $[\text{Ca}^{2+}]_i$ response by $337 \pm 43 \text{ nM}$ ($n = 11$; Fig. 5A). As shown by the arrows in Fig. 5A, a clearly visible $[\text{Ca}^{2+}]_i$ deflection was elicited by application of ruthenium red. The peak value of the ruthenium red-induced $[\text{Ca}^{2+}]_i$ response was $147 \pm 6\%$ ($n = 11$) of the initial control response ($P < 0.01$). A similar ruthenium red-induced $[\text{Ca}^{2+}]_i$ spike was also observed when Indo-1 was used as indicator ($n = 5$). Thus ruthenium red caused an increase in $[\text{Ca}^{2+}]_i$ that exceeded the NMDA-induced $[\text{Ca}^{2+}]_i$ response. Moreover, despite an increase in peak $[\text{Ca}^{2+}]_i$, ruthenium red did not impair the recovery of the $[\text{Ca}^{2+}]_i$ response. Following a 3 min exposure to ruthenium red, the NMDA-induced $[\text{Ca}^{2+}]_i$ response (R2 in Fig. 5A) had recovered by 95% ($n = 11$). This was not significantly different from control which had also recovered

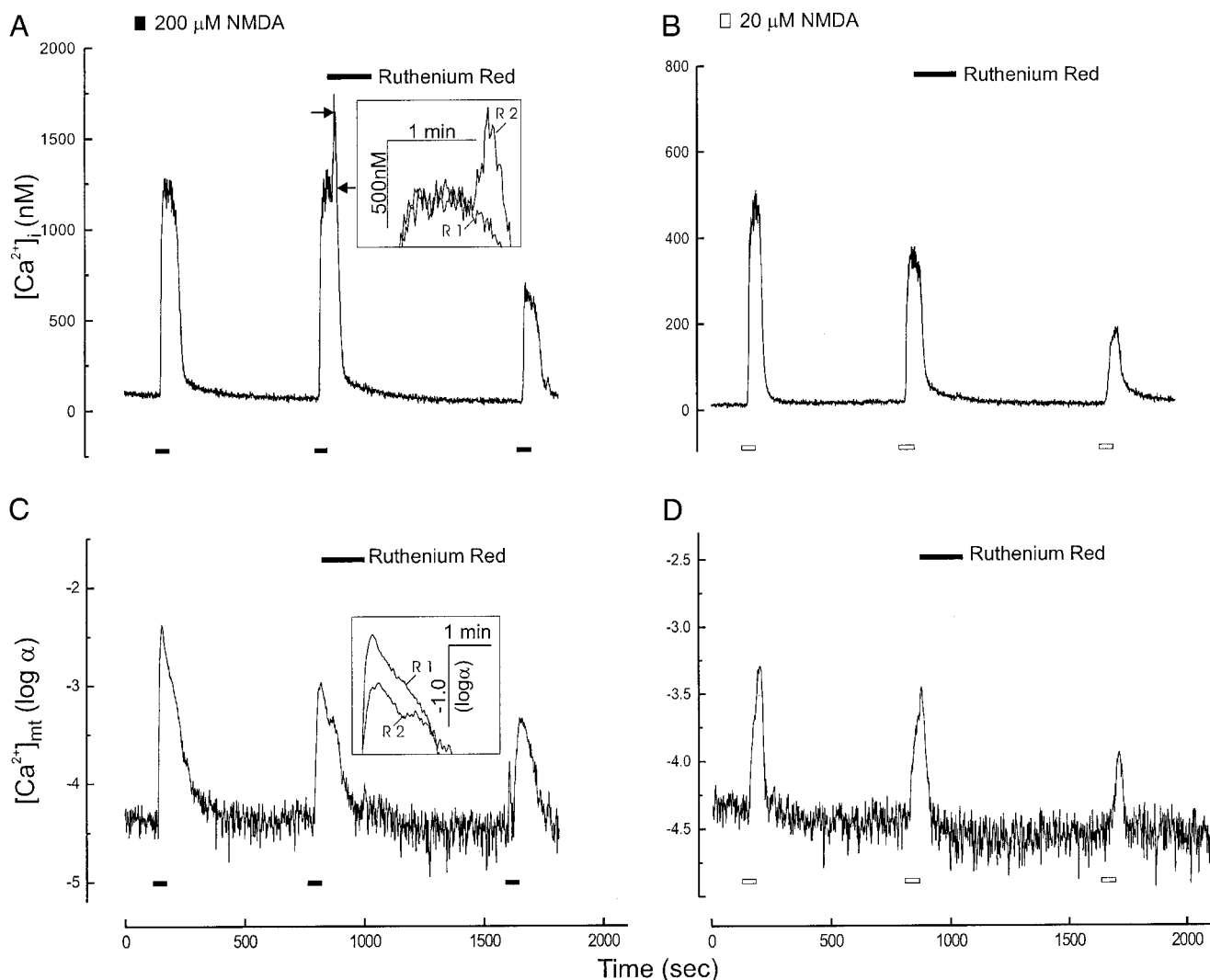


FIG. 5. Ruthenium red increased $[Ca^{2+}]_i$ following 200 μ M NMDA but not 20 μ M NMDA in hippocampal neurons. A: application of 100 μ M ruthenium red for 3 min following 200 μ M NMDA (60 s) evoked an increase in $[Ca^{2+}]_i$ (arrows). C: application of 100 μ M ruthenium red for 3 min following 200 μ M NMDA (60 s) did not cause an upstroke in $[Ca^{2+}]_{mt}$. Insets: the peak of response 1 (R1) overlaid on response 2 (R2). Ruthenium red did not cause an upstroke in $[Ca^{2+}]_i$ (B) or $[Ca^{2+}]_{mt}$ (D) following 20 μ M NMDA (60 s). $[Ca^{2+}]_i$ responses induced by 20 μ M and 200 μ M NMDA were recorded using Indo-1 and Indo-5F, respectively. $[Ca^{2+}]_{mt}$ was recorded as described in METHODS. Traces are representative of 5–11 recordings.

by 95% over 3 min ($n = 5$, Fig. 2A), suggesting that the increase in $[Ca^{2+}]_i$ induced by ruthenium red was not due to the impairment of Ca^{2+} extrusion mechanisms.

To further address this question, we tested the effect of ruthenium red on the 20 μ M NMDA-induced $[Ca^{2+}]_i$ response. As shown in Fig. 5B, application of 100 μ M ruthenium red for 3 min did not cause a further increase in $[Ca^{2+}]_i$ following the 20 μ M NMDA stimulus ($n = 5$, Fig. 5B), which was not significantly different from control cells (Fig. 3A; $P > 0.05$). Ruthenium red also failed to affect the response when Indo-5F was used as indicator ($n = 5$). This result suggested that like CGP 37157, the effect of ruthenium red depended on the size of the NMDA-induced Ca^{2+} load.

In addition to ruthenium red, we have performed experiments with RU360, an oxygen-bridged dinuclear ruthenium red derivative that is a more specific but more labile inhibitor of the mitochondrial Ca^{2+} uniporter (Matlib et al. 1998; Ying et al. 1991). In two of five cells, application of 100 μ M RU360

after 200 μ M NMDA stimulus produced a small, but clearly visible, increase in $[Ca^{2+}]_i$ over the 200 μ M NMDA-induced $[Ca^{2+}]_i$ responses. The reason why ruthenium red produced a more pronounced and more reproducible effect than RU 360 is likely due to the poor stability of RU 360. In spite of attempts to prevent its oxidation, we could not perform more than a single experiment from a vial of RU 360. Thus we carried out these studies with ruthenium red. To overcome the poor membrane permeability of this compound, we used a high drug concentration in a protocol in which nonselective effects on Ca^{2+} influx would not influence the outcome of the experiment.

Application of 100 μ M ruthenium red for 3 min following 200 μ M NMDA had no apparent effect on $[Ca^{2+}]_{mt}$ (Fig. 5C). Of particular interest was the absence of a $[Ca^{2+}]_{mt}$ upstroke on ruthenium red application ($n = 7$). The amplitude of the second $[Ca^{2+}]_{mt}$ response in ruthenium red-treated cells was $91 \pm 2\%$ ($n = 7$) of the first response (Fig. 5C), similar to that

recorded in untreated cells ($86 \pm 5\%$, $n = 6$; Fig. 2C). Because the same treatment induced a significant increase in $[\text{Ca}^{2+}]_i$ (Fig. 5A), this result suggests that ruthenium red blocked Ca^{2+} entry into mitochondria. Application of $100 \mu\text{M}$ ruthenium red for 3 min following $20 \mu\text{M}$ NMDA did not alter the $[\text{Ca}^{2+}]_{\text{mt}}$ response (Fig. 5D). The amplitude of the second $[\text{Ca}^{2+}]_{\text{mt}}$ response in ruthenium red-treated cells was $90 \pm 5\%$ ($n = 9$), similar to control ($93 \pm 4\%$, $n = 5$; Fig. 2D).

DISCUSSION

Isolated mitochondria bathed in micromolar concentrations of Ca^{2+} will take up and release calcium in a futile cycle that dissipates energy (Crompton and Heid 1978; Crompton et al. 1976). This is the first report to show that the futile cycle occurs in intact cells. This was made possible by recording Ca^{2+} levels in both the cytoplasm and the mitochondrial matrix in parallel. We find particularly compelling the observation that under conditions during which Ca^{2+} was purportedly cycling, that blocking Ca^{2+} uptake produced an effect opposite to that resulting from blocking Ca^{2+} release from the mitochondria. Furthermore, the blockers produced opposite effects on $[\text{Ca}^{2+}]_i$ versus the $[\text{Ca}^{2+}]_{\text{mt}}$. The Ca^{2+} recycling hypothesis uniquely predicts these reciprocal changes in Ca^{2+} levels within the two compartments.

We uncoupled mitochondria with FCCP in combination with oligomycin to functionally assess the mitochondrial localization of aequorin in hippocampal neurons. The mitochondrial poisons inhibited the $[\text{Ca}^{2+}]_{\text{mt}}$ response but enhanced the $[\text{Ca}^{2+}]_i$ response, confirming that in our experiments aequorin was successfully targeted to mitochondria. The FCCP-induced inhibition of the NMDA-induced $[\text{Ca}^{2+}]_{\text{mt}}$ response was not complete. FCCP inhibited the $20 \mu\text{M}$ NMDA-induced $[\text{Ca}^{2+}]_{\text{mt}}$ response by 76% and inhibited the $200 \mu\text{M}$ NMDA-induced $[\text{Ca}^{2+}]_{\text{mt}}$ response by 56%. The remaining FCCP-insensitive component of the $[\text{Ca}^{2+}]_{\text{mt}}$ response could result from a small contamination of cytosolic aequorin or Ca^{2+} may enter the mitochondria in the presence of FCCP and oligomycin driven by the large NMDA-induced Ca^{2+} gradient. Consistent with the later idea was the more complete FCCP-mediated inhibition of the $20 \mu\text{M}$ relative to the $200 \mu\text{M}$ NMDA-induced response. Although we cannot rule out the possibility of a small contamination of cytosolic aequorin in our cells, this contamination, if it exists, would not likely influence our conclusions because $[\text{Ca}^{2+}]_i$ and $[\text{Ca}^{2+}]_{\text{mt}}$ change in opposite directions in experiments with CGP 37157 and ruthenium red. However, aequorin in the cytoplasm could contribute to the inability to detect a decrease in $[\text{Ca}^{2+}]_{\text{mt}}$ during application of ruthenium red. Aequorin reconstituted with coelenterazine *f* is sensitive to Ca^{2+} changes between ~ 30 and $3,000 \text{ nM}$ (Shimomura et al. 1993). Some groups have estimated that $[\text{Ca}^{2+}]_{\text{mt}}$ reaches levels in the millimolar range near the mouths of Ca^{2+} channels (Montero et al. 2000). Thus it is possible that $[\text{Ca}^{2+}]_{\text{mt}}$ was under reported for some mitochondria possibly affecting the magnitude of the changes we described but not the primary conclusions.

CGP 37157 is an effective inhibitor of $\text{Na}^+/\text{Ca}^{2+}$ exchange across the inner mitochondrial membrane (Cox et al. 1993). We have noted that at concentrations needed to inhibit the exchanger in intact neurons that CGP 37157 also inhibits Ca^{2+} influx across the plasma membrane (Baron and Thayer 1997)

consistent with its benzothiazepine (diltiazem-like) structure (Cox et al. 1993). Thus the most effective protocols for using CGP 37157 in intact cells apply the drug after the stimulus and Ca^{2+} influx has ceased (White and Reynolds 1997). We attribute the effects of CGP 37157 on the $200 \mu\text{M}$ NMDA-induced response to its inhibition of mitochondrial $\text{Na}^+/\text{Ca}^{2+}$ exchange during Ca^{2+} recycling across the inner membrane. CGP 37157 trapped Ca^{2+} inside the mitochondrion, preventing it from contributing to the cytosolic Ca^{2+} pool and thus accelerating the recovery of $[\text{Ca}^{2+}]_i$. Ca^{2+} release from mitochondria into the cytosol resumed after removal of CGP 37157, resulting in a secondary rise in $[\text{Ca}^{2+}]_i$. In parallel experiments in which intramitochondrial calcium was measured by mitochondrially targeted aequorin, CGP 37157 was shown to prolong the recovery of the $[\text{Ca}^{2+}]_{\text{mt}}$ response, confirming that the effects of CGP 37157 on $[\text{Ca}^{2+}]_i$ were indeed due to its inhibition of mitochondrial $\text{Na}^+/\text{Ca}^{2+}$ exchange. Moreover, we showed that the effects of CGP 37157 were dependent on the intensity of the NMDA stimulus. The drug produced pronounced effects on $200 \mu\text{M}$ NMDA-induced $[\text{Ca}^{2+}]_i$ and $[\text{Ca}^{2+}]_{\text{mt}}$ responses but did not cause a detectable change in responses evoked by $20 \mu\text{M}$ NMDA. Presumably, mitochondria act in the " Ca^{2+} uptake mode" when challenged with the more modest $20 \mu\text{M}$ NMDA stimulus (Colegrove et al. 2000a). Larger NMDA-evoked Ca^{2+} loads evoked greater Ca^{2+} recycling across the inner mitochondrial membrane.

Ruthenium red is an effective inhibitor of the mitochondrial uniporter (Moore 1971). The drug was applied after the NMDA stimulus to avoid nonspecific effects on Ca^{2+} influx pathways and to study its actions after the establishment of a large Ca^{2+} load. Application of ruthenium red following $200 \mu\text{M}$ NMDA evoked a transient upstroke in $[\text{Ca}^{2+}]_i$. This increase in $[\text{Ca}^{2+}]_i$ did not result from Ca^{2+} influx because $100 \mu\text{M}$ ruthenium red had no effect on $20 \mu\text{M}$ NMDA-induced $[\text{Ca}^{2+}]_i$ responses and tends to block, not activate, Ca^{2+} permeable channels. Ruthenium red did not appear to affect plasmalemma Ca^{2+} extrusion mechanisms, such as the Ca^{2+} -ATPase and $\text{Na}^+/\text{Ca}^{2+}$ exchanger, because after the initial ruthenium red-induced $[\text{Ca}^{2+}]_i$ upstroke, recovery of $[\text{Ca}^{2+}]_i$ was not impaired. The lack of effect on the $20 \mu\text{M}$ NMDA-induced response also argues for action on low-affinity mitochondrial Ca^{2+} buffering. However, inhibition of Ca^{2+} efflux across the plasmalemma would be predicted to increase $[\text{Ca}^{2+}]_i$ during continued release of Ca^{2+} from an intracellular store such as the mitochondrion. Ruthenium red is known to inhibit Ca^{2+} release from the endoplasmic reticulum via the ryanodine receptor (Xu et al. 1999) although it is unlikely that blocking Ca^{2+} -induced Ca^{2+} release could produce an increase in $[\text{Ca}^{2+}]_i$. There are precedents for using ruthenium red to inhibit the uniporter in intact cells. Application of $150 \mu\text{M}$ ruthenium red to a hippocampal cell line treated with glutamate reduced the production of reactive oxygen species and improved survival (Tan et al. 1998). Ruthenium red was shown to selectively block the mitochondrial uniporter in intact cardiac myocytes at $10 \mu\text{M}$ if sufficient time was allowed for the poorly permeant drug to enter the cell (Trollinger et al. 2000). The Ca^{2+} recycling hypothesis predicts that ruthenium red would accelerate the recovery of $[\text{Ca}^{2+}]_{\text{mt}}$ in the paradigm used in this study. Our failure to observe this change might result from Ca^{2+} buffering in the matrix, the brevity of the response, or simply the difficulty in quantifying subtle in-

creases in $[Ca^{2+}]_{mt}$ recovery kinetics. The results presented here demonstrate that Ca^{2+} entry and release from mitochondria occur simultaneously and that this process was more pronounced following exposure to high concentrations of NMDA.

The effects of CGP 37157 and ruthenium red were observed in hippocampal neurons treated with 200 μ M NMDA but not in neurons treated with 20 μ M NMDA. Mitochondria take up significant Ca^{2+} into the matrix in response to both stimuli but recycling was only apparent following 200 μ M NMDA. This observation is consistent with mitochondria exhibiting net uptake following 20 μ M NMDA and simultaneous Ca^{2+} uptake and release following 200 μ M NMDA. These observations are consistent with a computer model of mitochondrial Ca^{2+} transport (Colegrove et al. 2000b). Because 200 μ M NMDA is toxic to neurons, whereas 20 μ M NMDA is much less toxic (Sattler et al. 1999), the results are consistent with the idea that Ca^{2+} recycling across the mitochondrial inner membrane contributes to NMDA-induced neurotoxicity. This conclusion is supported by experiments with isolated mitochondria that found that Ca^{2+} cycled across the inner membrane only when mitochondria were exposed to large, potentially toxic Ca^{2+} levels (Crompton et al. 1976).

In cells that are exposed to glutamate or NMDA, Ca^{2+} recycling across the mitochondrial inner membrane might occur continuously. The rapid uptake and release of Ca^{2+} into the matrix allows increased energy demands signaled by increases in $[Ca^{2+}]_i$ to stimulate ATP production via dehydrogenases that sense $[Ca^{2+}]_{mt}$ (McCormack et al. 1990). However, the physiological role of continuous recycling of Ca^{2+} across the inner membrane is less clear. We observed recycling only when large potentially toxic Ca^{2+} loads were applied to hippocampal neurons suggesting that it may be a pathological process. A futile recycling of Ca^{2+} dissipates energy in isolated mitochondria (Moore 1971) although the magnitude of the energy drain in intact cells is not known. Both ATP depletion and the production of reactive oxygen species have been detected in neurons exposed to glutamate and NMDA (Ankarcrona et al. 1995; Lafon-Cazal et al. 1993), although the reasons for these changes are not certain. Na^+ -induced Ca^{2+} release from neuronal mitochondria during hypoxia suggests a mitochondrial contribution to stroke damage (Zhang and Lipton 1999). Increased production of superoxide by the mitochondrial electron transport chain may be responsible for hyperglycemia-induced tissue damage (Nishikawa et al. 2000). These studies suggest that mitochondria contribute to toxicity in an active way, an idea supported by the temporary protection from glutamate-induced necrosis afforded by dissipating the mitochondrial membrane potential (Nicholls and Ward 2000; Stout et al. 1998).

In conclusion, NMDA-induced Ca^{2+} loads were taken up and released across the mitochondrial inner membrane in hippocampal neurons, creating a futile Ca^{2+} cycle. The Ca^{2+} recycling process was associated with a toxic concentration of NMDA and may contribute to glutamate-induced neuronal death. Mitochondrial Ca^{2+} cycling might deplete ATP and generate toxic concentrations of reactive oxygen species. The elaborate Ca^{2+} transport system in the mitochondrion provides numerous potential targets for pharmacologic intervention in glutamate neurotoxicity.

We thank K. T. Baron and R. A. Padua for initial work on establishing the method for measuring intramitochondrial calcium.

This work was supported by National Institute on Drug Abuse Grants DA-7304 and DA-11806 and by National Science Foundation Grant IBN0110409.

REFERENCES

- ANKARCORONA M, DYPBUKT JM, BONFOCO E, ZHIVOTOVSKY B, ORRENIUS S, LIPTON SA, AND NICOTERA P. Glutamate-induced neuronal death—a succession of necrosis or apoptosis depending on mitochondrial function. *Neuron* 15: 961–973, 1995.
- BARON KT AND THAYER SA. CGP37157 modulates mitochondrial Ca^{2+} homeostasis in cultured rat dorsal root ganglion neurons. *Eur J Pharmacol* 340: 295–300, 1997.
- BLAUSTEIN MP, RATZLAFF RW, AND KENDRICK NK. The regulation of intracellular calcium in presynaptic nerve terminals. *Ann NY Acad Sci* 307: 195–212, 1978.
- BOHN MC, CHOI-LUNDBERG DL, DAVIDSON BL, LERANTH C, KOZLOWSKI DA, SMITH JC, O'BANION MK, AND REDMOND DE JR. Adenovirus-mediated transgene expression in nonhuman primate brain. *Hum Gene Ther* 10: 1175–1184, 1999.
- CASTILHO RF, WARD MW, AND NICHOLLS DG. Oxidative stress, mitochondrial function, and acute glutamate excitotoxicity in cultured cerebellar granule cells. *J Neurochem* 72: 1394–1401, 1999.
- CHACON E AND ACOSTA D. Mitochondrial regulation of superoxide by Ca^{2+} : an alternate mechanism for the cardiotoxicity of doxorubicin. *Toxicol Appl Pharmacol* 107: 117–128, 1991.
- COBBOLD PH AND LEE JAC. Aequorin measurements of cytoplasmic free calcium. In: *Cellular Calcium; A Practical Approach*, edited by McCormack JG and Cobbold PH. New York: Oxford, 1991, p. 55–81.
- COLEGROVE SL, ALBRECHT MA, AND FRIEL DD. Dissection of mitochondrial Ca^{2+} uptake and release fluxes in situ after depolarization-evoked $[Ca^{2+}]_i$ elevations in sympathetic neurons. *J Gen Physiol* 115: 351–369, 2000a.
- COLEGROVE SL, ALBRECHT MA, AND FRIEL DD. Quantitative analysis of mitochondrial Ca^{2+} uptake and release pathways in sympathetic neurons—reconstruction of the recovery after depolarization-evoked $[Ca^{2+}]_i$ elevations. *J Gen Physiol* 115: 371–388, 2000b.
- COX DA, CONFORTI L, SPERELAKIS N, AND MATLIB MA. Selectivity of inhibition of Na^+ - Ca^{2+} exchange of heart mitochondria by benzothiazepine CGP-37157. *J Cardiovasc Pharmacol* 21: 595–599, 1993.
- CROMPTON M AND HEID I. The cycling of calcium, sodium, and protons across the inner membrane of cardiac mitochondria. *Eur J Biochem* 91: 599–608, 1978.
- CROMPTON M, SIGEL E, SALZMANN M, AND CARAFOLI E. The sodium-induced efflux of calcium from heart mitochondria. *Eur J Biochem* 69: 429–434, 1976.
- DAVID G. Mitochondrial clearance of cytosolic Ca^{2+} in stimulated lizard motor nerve terminals proceeds without progressive elevation of mitochondrial matrix $[Ca^{2+}]$. *J Neurosci* 19: 7495–7506, 1999.
- DUCHEN MR. Contributions of mitochondria to animal physiology: from homeostatic sensor to calcium signalling and cell death. *J Physiol (Lond)* 516: 1–17, 1999.
- FRIEL DD AND TSIEH RW. An FCCP-sensitive Ca^{2+} store in bullfrog sympathetic neurons and its participation in stimulus-evoked changes in $[Ca^{2+}]_i$. *J Neurosci* 14: 4007–4024, 1994.
- GRIFFITHS EJ. Use of ruthenium red as an inhibitor of mitochondrial Ca^{2+} uptake in single rat cardiomyocytes. *FEBS Lett* 486: 257–260, 2000.
- GUNTER T, GUNTER K, SHEU S, AND GAVIN C. Mitochondrial calcium transport: physiological and pathological relevance. *Am J Physiol Cell Physiol* 267: C313–C339, 1994.
- ICHAS F AND MAZAT JP. From calcium signaling to cell death: two conformations for the mitochondrial permeability transition pore. Switching from low- to high-conductance state. *Biochim Biophys Acta* 1366: 33–50, 1998.
- LAFON-CAZAL M, PIETRI S, CULCASI M, AND BOCKAERT J. NMDA-dependent superoxide production and neurotoxicity. *Nature* 364: 535–537, 1993.
- LEHNINGER AL. Energy coupling in electron transport. *Fed Proc* 26: 1333–1334, 1967.
- MALECOT CO, BITO V, AND ARGIBAY JA. Ruthenium red as an effective blocker of calcium and sodium currents in guinea-pig isolated ventricular heart cells. *Br J Pharmacol* 124: 465–472, 1998.
- MATLIB MA, ZHOU Z, KNIGHT S, AHMED S, CHOI KM, KRAUSEBAUER J, PHILLIPS R, ALTSCHULD R, KATSUBE Y, SPERELAKIS N, AND BERS DM.

- Oxygen-bridged dinuclear ruthenium amine complex specifically inhibits Ca^{2+} uptake into mitochondria in vitro and in situ in single cardiac myocytes. *J Biol Chem* 273: 10223–10231, 1998.
- McCORMACK JG, HALESTRAP AP, AND DENTON RM. Role of calcium ions in regulation of mammalian intramitochondrial metabolism. *Physiol Rev* 70: 391–425, 1990.
- MILLER JR. Mitochondria—the Kraken wakes! *Trends Neurosci* 21: 95–97, 1998.
- MONTERO M, ALONSO MT, CARNICERO E, CUCHILLO-IBANEZ I, ALBILLOS A, GARCIA AG, GARCIA-SANCHO J, AND ALVAREZ J. Chromaffin-cell stimulation triggers fast millimolar mitochondrial Ca^{2+} transients that modulate secretion. *Nat Cell Biol* 2: 57–61, 2000.
- MOORE CL. Specific inhibition of mitochondrial Ca^{2+} transport by ruthenium red. *Biochem Biophys Res Commun* 42: 298–305, 1971.
- NICHOLLS DG AND FERGUSON SJ. Secondary transport. In: *Bioenergetics* (2nd ed.), edited by Nicholls DG and Ferguson SJ. London: Academic, 1992, p. 207–234.
- NICHOLLS DG AND WARD MW. Mitochondrial membrane potential and neuronal glutamate excitotoxicity: mortality and millivolts. *Trends Neurosci* 23: 166–174, 2000.
- NISHIKAWA T, EDELSTEIN D, DU XL, YAMAGISHI S, MATSUMURA T, KANEDA Y, YOREK MA, BEEBE D, OATES PJ, HAMMES HP, GIARDINO I, AND BROWNLEE M. Normalizing mitochondrial superoxide production blocks three pathways of hyperglycaemic damage. *Nature* 404: 787–790, 2000.
- PADUA RA, BARON KT, THYAGARAJAN B, CAMPBELL C, AND THAYER SA. Reduced Ca^{2+} uptake by mitochondria in pyruvate dehydrogenase-deficient human diploid fibroblasts. *Am J Physiol Cell Physiol* 43: C615–C622, 1998.
- PENG TI AND GREENAMYRE JT. Privileged access to mitochondria of calcium influx through N-methyl-D-aspartate receptors. *Mol Pharmacol* 53: 974–980, 1998.
- RIZZUTO R, BRINI M, MURGIA M, AND POZZAN T. Microdomains with high Ca^{2+} close to IP_3 -sensitive channels that are sensed by neighboring mitochondria. *Science* 262: 744–747, 1993.
- RIZZUTO R, PINTON P, CARRINGTON W, FAY FS, FOGARTY KE, LIFSHITZ LM, TUFT RA, AND POZZAN T. Close contacts with the endoplasmic reticulum as determinants of mitochondrial Ca^{2+} responses. *Science* 280: 1763–1766, 1998.
- SATTLER R, XIONG Z, LU WY, HAFNER M, MACDONALD JF, AND TYMIANSKI M. Specific coupling of NMDA receptor activation to nitric oxide neurotoxicity by PSD-95 protein. *Science* 284: 1845–1848, 1999.
- SHIMOMURA O, MUSICKI B, KISHI Y, AND INOUE S. Light-emitting properties of recombinant semi-synthetic aequorins and recombinant fluorescein-conjugated aequorin for measuring cellular calcium. *Cell Calcium* 14: 373–378, 1993.
- STOUT AK, RAPHAEL HM, KANTEREWICZ BI, KLANN E, AND REYNOLDS IJ. Glutamate-induced neuron death requires mitochondrial calcium uptake. *Nat Neurosci* 1: 366–373, 1998.
- TAN S, SAGARA Y, LIU Y, MAHER P, AND SCHUBERT D. The regulation of reactive oxygen species production during programmed cell death. *J Cell Biol* 141: 1423–1432, 1998.
- TANG YG AND ZUCKER RS. Mitochondrial involvement in post-tetanic potentiation of synaptic transmission. *Neuron* 18: 483–491, 1997.
- THAYER SA AND MILLER RJ. Regulation of the free intracellular calcium concentration in rat dorsal root ganglion neurones in vitro. *J Physiol (Lond)* 425: 85–115, 1990.
- THAYER SA, STUREK M, AND MILLER RJ. Measurement of neuronal Ca^{2+} transients using simultaneous microfluorimetry and electrophysiology. *Pflügers Arch* 412: 216–223, 1988.
- TROLLINGER DR, CASCIO WE, AND LEMASTERS JJ. Mitochondrial calcium transients in adult rabbit cardiac myocytes: inhibition by ruthenium red and artifacts caused by lysosomal loading of Ca^{2+} -indicating fluorophores. *Biophys J* 79: 39–50, 2000.
- VELASCO I AND TAPIA R. Alterations of intracellular calcium homeostasis and mitochondrial function are involved in ruthenium red neurotoxicity in primary cortical cultures. *J Neurosci Res* 60: 543–551, 2000.
- WANG GJ, CHUNG HJ, SCHNUR J, LEA E, ROBINSON MB, POTTHOFF WK, AIZENMAN E, AND ROSENBERG PA. Dihydrokainate-sensitive neuronal glutamate transport is required for protection of rat cortical neurons in culture against synaptically released glutamate. *Eur J Neurosci* 10: 2523–2531, 1998.
- WANG GJ, RANDALL RD, AND THAYER SA. Glutamate-induced intracellular acidification of cultured hippocampal neurons demonstrates altered energy metabolism resulting from Ca^{2+} loads. *J Neurophysiol* 72: 2563–2569, 1994.
- WANG GJ AND THAYER SA. Sequestration of glutamate-induced Ca^{2+} loads by mitochondria in cultured rat hippocampal neurons. *J Neurophysiol* 76: 1611–1621, 1996.
- WERTH JL AND THAYER SA. Mitochondria buffer physiological calcium loads in cultured rat dorsal root ganglion neurons. *J Neurosci* 14: 348–356, 1994.
- WHITE R AND REYNOLDS I. Mitochondria and $\text{Na}^+/\text{Ca}^{2+}$ exchange buffer glutamate-induced calcium loads in cultured cortical neurons. *J Neurosci* 15: 1318–1328, 1995.
- WHITE RJ AND REYNOLDS IJ. Mitochondria accumulate Ca^{2+} following intense glutamate stimulation of cultured rat forebrain neurones. *J Physiol (Lond)* 498: 31–47, 1997.
- XU L, TRIPATHY A, PASEK DA, AND MEISSNER G. Ruthenium red modifies the cardiac and skeletal muscle Ca^{2+} release channels (ryanodine receptors) by multiple mechanisms. *J Biol Chem* 274: 32680–32691, 1999.
- YING W-L, EMERSON J, CLARKE MJ, AND SANADI DR. Inhibition of mitochondrial calcium ion transport by an oxo-bridged dinuclear ruthenium amine complex. *Biochemistry* 30: 4949–4952, 1991.
- ZHANG Y AND LIPTON P. Cytosolic Ca^{2+} changes during in vitro ischemia in rat hippocampal slices: major roles for glutamate and Na^+ -dependent Ca^{2+} release from mitochondria. *J Neurosci* 19: 3307–3315, 1999.